JACS
JOURNAL OF THE AMERICAN CHEMICAL SOCIETY

Article

pubs.acs.org/JACS

# W-Band Time-Resolved Electron Paramagnetic Resonance Study of Light-Induced Spin Dynamics in Copper−Nitroxide-Based Switchable Molecular Magnets

Matvey V. Fedin,*[,†] Elena G. Bagryanskaya,*[,†,§] Hideto Matsuoka,[‡] Seigo Yamauchi,[‡] Sergey L. Veber,[†] Ksenia Yu. Maryunina,[†] Evgeny V. Tretyakov,[†] Victor I. Ovcharenko,[†] and Renad Z. Sagdeev[†]

[†]International Tomography Center SB RAS, Institutskaya str. 3a, 630090 Novosibirsk, Russia

[§]N.N. Vorozhtsov Novosibirsk Institute of Organic Chemistry SB RAS, Pr. Lavrentjeva 9, 630090 Novosibirsk, Russia

[‡]Institute of Multidisciplinary Research for Advanced Materials, Tohoku University, Katahira 2-1-1, Aoba-ku, Sendai 980-8577, Japan

Supporting Information

**ABSTRACT:** Molecular magnets $Cu(hfac)_2L^R$ represent a new type of photoswitchable materials based on exchange-coupled clusters of copper(II) with stable nitroxide radicals. It was found recently that the photoinduced spin state of these compounds is metastable on the time scale of hours at cryogenic temperatures, similar to the light-induced excited spin state trapping phenomenon well-known for many spin-crossover compounds. Our previous studies have shown that electron paramagnetic resonance (EPR) in continuous wave (CW) mode allows for studying the light-induced spin state conversion and relaxation in the $Cu(hfac)_2L^R$ family. However, light-induced spin dynamics in these compounds has not been studied on the sub-second time scale so far. In this work we report the first time-resolved (TR) EPR study of light-induced spin state switching and relaxation in $Cu(hfac)_2L^R$ with nanosecond temporal resolution. To enhance spectral resolution we used high-frequency TR EPR at W-band (94 GHz). We first discuss the peculiarities of applying TR EPR to the solid-phase compounds $Cu(hfac)_2L^R$ at low (liquid helium) temperatures and approaches developed for photoswitching/relaxation studies. Then we analyze the kinetics of the excited spin state at $T$ = 5−21 K. It has been found that the photoinduced spin state is formed at time delays shorter than 100 ns. It has also been found that the observed relaxation of the excited state is exponential on the nanosecond time scale, with the decay rate depending linearly on temperature. We propose and discuss possible mechanisms of these processes and correlate them with previously obtained CW EPR data.

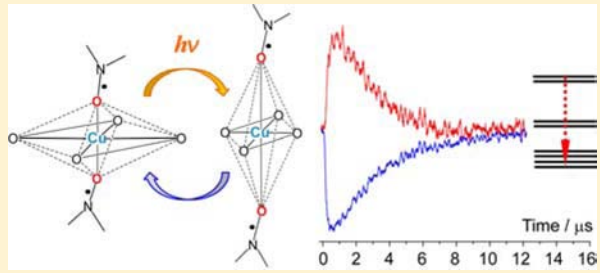


## INTRODUCTION

Photoswitchable molecular compounds are intensively studied for various potential applications in nanotechnology, e.g., as switching devices and sensors and as elementary units for data storage and processing.[1−5] Among them, systems with the switching of electron spins have attracted special interest.[4−7] Spin-crossover (SCO) compounds based on 3d-metals are, perhaps, the most well-known and well-studied materials exhibiting switching between high-spin (HS) and low-spin (LS) states induced by temperature or light.[4,5,8−17] Spin-Peierls state switching in charge-transfer compounds is the other example that shows promise for spintronics.[18] Recently, thermally induced and light-induced magnetic anomalies somewhat similar to those observed for both SCO compounds and spin-Peierls systems were found for polymer-chain compounds $Cu(hfac)_2L^R$, based on copper(II) hexafluoroacetylacetonates ($Cu(hfac)_2$) bridged by stable nitroxide radicals ($L^R$).[19−27] These systems exhibit highly cooperative reversible switching between strongly exchange-coupled and weakly exchange-coupled spin states (SS and WS states, respectively) of spin triads nitroxide−copper(II)−nitroxide. Because of the large difference in bond lengths between SS and WS state (unit cell volume changes by up to 13%) and the high mechanical stability during switching, these crystals have been described as "breathing". Apart from breathing crystals, several other examples (including very recent ones) of interesting magnetic behavior in compounds based on copper(II) and/or nitroxides have been reported.[28−34]

Electron paramagnetic resonance (EPR) is sensitive to the SS↔WS states switching in breathing crystals. We used multifrequency EPR in a series of recent works to detect spin state switching induced by temperature or light.[22−27] Similar to the light-induced excited spin state trapping (LIESST) phenomenon well-known for iron(II) SCO compounds,[9,10] the light-induced WS state in breathing crystals is metastable on the time scale of hours at cryogenic temperatures.[26,27] Recently we have studied the relaxation of the light-induced WS state to the ground SS state in several compounds of the family of breathing crystals.[27] It was found that the relaxation strongly

**Received:** July 3, 2012
**Published:** September 10, 2012

   dx.doi.org/10.1021/ja306467e | J. Am. Chem. Soc. 2012, 134, 16319−16326

deviates from monoexponential behavior and is self-decelerating due to the broad distribution of relaxation rates in exchange-coupled clusters. On the other hand, to date, little is understood about the mechanism of photoswitching and spin dynamics on the short time scale, since temporal resolution of conventional continuous wave (CW) EPR does not allow one to monitor fast processes on sub-minute time scales. This paper reports the first time-resolved (TR) EPR study of breathing crystals. TR EPR is most often used for studying photoinduced reactions in liquids at ambient temperatures or in frozen solutions;[35−52] however, as we show here, it can also be used for monitoring transient EPR signals in solid-phase molecular magnets arising during spin state switching/relaxation on the nanosecond time scale. To enhance spectral resolution, we use high-field W-band TR EPR (94 GHz). In the following sections we describe the specifics of application of TR EPR for photoswitching and relaxation studies in breathing crystals, investigate TR EPR kinetics of the excited spin state, and propose and discuss possible mechanisms for the observed relaxation.

## EXPERIMENTAL SECTION

In this study we used the compound $Cu(hfac)_2L^{Pr}$ (R = Pr, see Figure 1a), which has proven to be very robust against destruction during sample preparation and illumination with light,[26,27] and therefore is the best choice for the first TR EPR study of breathing crystals. Its synthesis, structure, magnetic properties, and EPR data were published previously[53,19,22] and are briefly summarized in the Supporting Information. $Cu(hfac)_2L^{Pr}$ exhibits a gradual thermal spin transition between $T \approx 100$ and 300 K. LIESST-like behavior under illumination with light was previously observed at $T < 20$ K.[26,27]

The compound $Cu(hfac)_2L^{Pr}$ has a very intense absorption in UV−vis−near-IR regions, with extinction coefficients of up to a few thousand $M^{-1}$ $cm^{-1}$ at 400−700 nm (in hexane). For the absorption measurement of the solid-phase compound, a thin microcrystalline film of $Cu(hfac)_2L^{Pr}$ embedded in poly(vinyl chloride) (PVC) was prepared (EPR identification is given in the Supporting Information). Temperature-dependent absorption measurements were carried out using a Bruker Vertex 80v FTIR spectrometer equipped with a cryostat and extension for UV−vis spectral regions.

Samples for EPR experiments were prepared using the same approach as in ref 26. To make the illumination efficient, crystals were ground, mixed with an excess of glass-forming liquid (glycerol) to form a suspension, and then frozen at cryogenic temperatures. *In situ* illumination at 532 nm was accomplished with a frequency-doubled Nd:YAG laser (Spectra Physics PRO270) using an optical fiber fed into the W-band sample capillary. The laser pulse repetition frequency was set to 20 Hz, and the output energy was attenuated to a maximum of 0.3 mJ on the sample surface. W-band transient EPR measurements were carried out using a Bruker E600 spectrometer. Temperature was controlled by an Oxford ER4112HV helium temperature control system. Simulations shown in Figure 4b were done using EasySpin toolbox for Matlab.[54]

## RESULTS AND DISCUSSION

**Spin States and Switching between Them in a Nitroxide−Copper(II)−Nitroxide Triad.** EPR spectra of WS and SS states in spin triads of breathing crystals have been studied in detail in our previous work.[22,55,56] Figure 1a shows the structure of polymer chains in the compound $Cu(hfac)_2L^{Pr}$, which consist of alternating spin triads (Cu1 ions coordinated by two nitroxides) and magnetically isolated Cu2 units. Figure 1b sketches the potential energy surface of breathing crystals and corresponding structures. It is very well established that at low temperatures, below spin transition, the SS state is the ground state.[55] In this state copper spin is

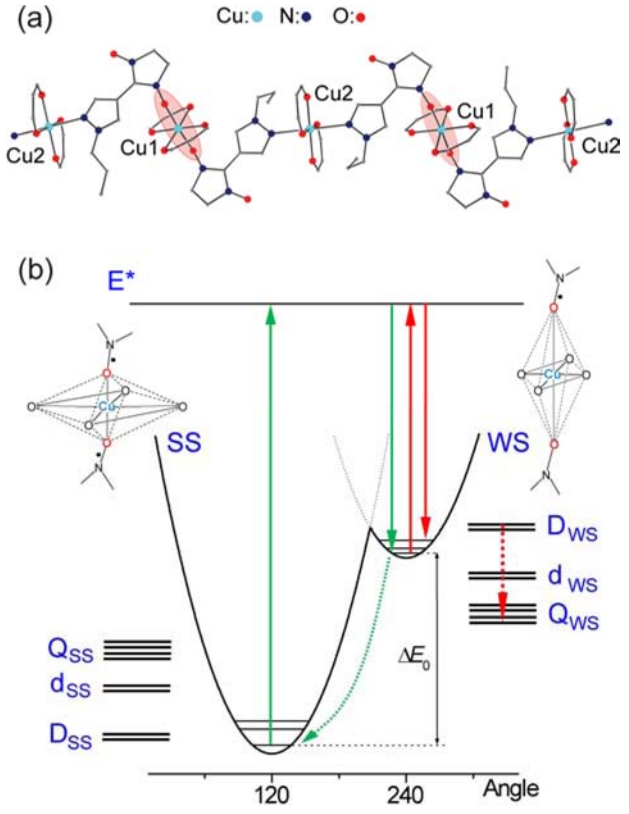


**Figure 1.** (a) Chemical structure of polymer chains of the switchable molecular magnets $Cu(hfac)_2L^{Pr}$; spin triads are circled. (b) Schematic circular section of the potential energy surface associated with the two Jahn−Teller valleys in breathing crystals. Spin level diagrams for the lowest vibronic states and structures corresponding to spin triad in SS and WS states are sketched on the left and on the right. Green and red arrows illustrate direct and secondary conversion pathways, respectively. Dotted green line shows tunneling relaxation from photoinduced WS to the ground SS state. Dotted red line shows electron spin relaxation in the WS state potential well observed by TR EPR.

coupled to each of the nitroxide spins by a strong antiferromagnetic exchange interaction, $J \approx -100$−200 $cm^{-1}$;[23] therefore, only the lowest doublet ($D_{SS}$) is populated. There are also excited doublet and quartet states in the spin triad, denoted $d_{SS}$ and $Q_{SS}$, respectively (Figure 1b). At high temperatures, above spin transition, the system is found in the WS state.[55] It is known that exchange coupling in the spin triad in the WS state becomes weak ($|J| \approx 10$−20 $cm^{-1}$).[25,23] There has been no direct evidence up to now that this coupling is ferromagnetic, since its magnitude is comparable with that of the intercluster/intermolecular exchange interactions, and also because at high temperatures $kT > J$ and all spin multiplets are populated. But, it is a very reasonable assumption, which follows from mutual location of electron orbitals and observations made elsewhere for similar structures.[57] Thus, the order of spin levels in a triad is reversed for the WS state, as shown in Figure 1b.

The photoswitching from SS to WS state can be induced in breathing crystals at low temperatures (typically below 20 K).[26,27] Figure 2 shows the absorption spectra of the studied compound at $T$ = 80−300 K. At high temperatures the spectrum is dominated by absorption bands of nitronyl nitroxide. (Broad absorption band of the copper(II) ions centered around 700 nm is much weaker and not visible at this


dx.doi.org/10.1021/ja306467e | J. Am. Chem. Soc. 2012, 134, 16319−16326

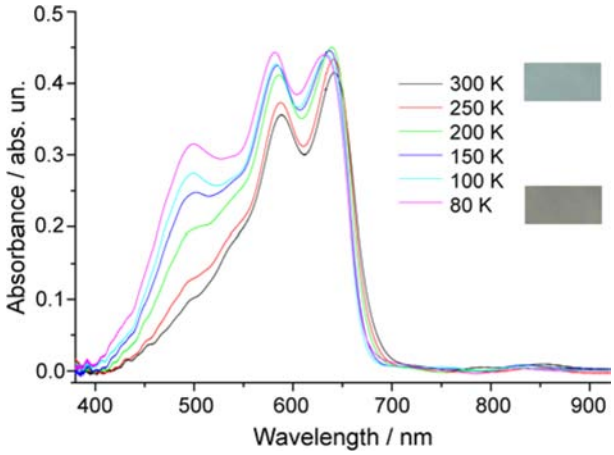


**Figure 2.** UV−vis absorption spectra of $Cu(hfac)_2L^{Pr}$ (embedded in PVC film) at $T$ = 80−300 K (indicated in the legend). Thermochromism is illustrated by photos of the film (violet-gray at $T$ = 80 K and bluish-gray at $T$ = 300 K) on the right.

optical density.) As the temperature is decreased, a strong absorption band with maximum at $\lambda_{max} \approx 500$ nm appears. We assign this band to the metal−ligand charge transfer (MLCT) transition, since its appearance at low temperatures correlates with the strong shortening of copper−nitroxide distances by ~0.3 Å.[19,22]

The mechanism of photoswitching is far from being fully understood to date, but it seems to be generally similar to the light-induced switching in SCO compounds. The excitation occurs via MLCT or d−d (for $\lambda$ > 700 nm) band to the intermediate excited state (or group of states which are generally referred to as E* in Figure 1b), from which relaxation leads to the intersystem crossing to the metastable WS state. Relaxation from WS to the ground SS state is contributed by tunneling and thermally activated processes and was studied on the time scale of minutes to hours using CW EPR.[27] It was therefore hoped that TR EPR experiment may provide more detailed information about the mechanisms of photoswitching and relaxation on the nanosecond time scale.

**TR EPR Signal: Origin and Contributions.** The TR EPR experiment (Figure 3a) is carried out without modulation of external magnetic field and phase-sensitive detection. As a result, first, the spectra are detected in an absorption shape instead of derivative-like shape observed in conventional CW EPR. Second, the absolute sensitivity of TR EPR is much lower compared to that of CW EPR, and usually TR EPR signal can only be observed for strongly spin-polarized systems. In addition, all time-independent contributions to the transient signal arising after the laser flash are removed by high-pass filtration; therefore, steady-state EPR signals are not observed.

Most often, TR EPR is applied in studies of photochemical reactions in liquids, where transient spin-polarized paramagnetic species are induced by a laser.[36,37] In breathing crystals one would not expect to detect spin polarization (manifested in enhanced absorption or emission) using TR EPR, since the electron relaxation times are extremely short due to the large exchange couplings operating in and between spin triads. In particular, electron spin echo cannot be observed in breathing crystals down to 4 K, and microwave power saturation is also never achieved. On the other hand, photoswitching between corresponding spin states in breathing crystals should lead to the fast transformation of the CW EPR

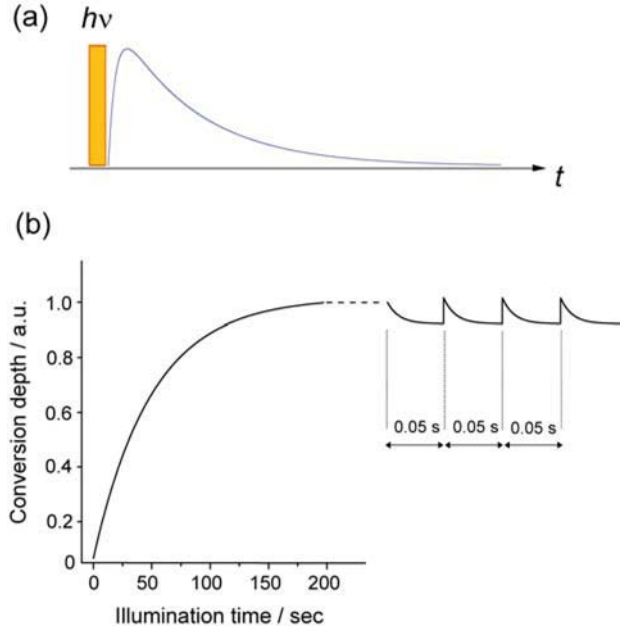


**Figure 3.** (a) Temporal diagram of the TR EPR experiment: transient signal is observed after application of the laser pulse. (b) Illustration of TR EPR in the study of SS→WS state conversion in breathing crystals. Quasi-stationary state is reached typically in 3−5 min after beginning illumination, then every laser flash converts some small fraction of SS state into WS state, which relaxes to a small extent before the next flash generates the next cycle. The amplitude of periodic changes of conversion depth is strongly magnified for clarity.

spectrum and, consequently, to the onset of transient TR EPR signal. In this case all observed signals are measured in Boltzman equilibrium within each spin multiplet, and the use of high-field W-band EPR leads to significant increase of the sensitivity. In addition, the two following peculiarities may be envisioned.

First, we have found previously that (i) conversion of the sample from SS to WS state under laser pulse illumination develops during several minutes, and (ii) complete relaxation from light-induced WS state to the ground SS state occurs on the time scale of hours at $T$ < 20 K.[26,27] On the one hand, accumulation of signals in TR EPR takes at least several minutes, i.e., enough time for the spin system to convert from SS to WS state. On the other hand, having a laser shot repetition rate of 20 Hz, clearly, only a tiny amount of WS states are allowed to relax within this 0.05 s interpulse delay. Therefore, during the TR EPR experiment, the spin system oscillates around some quasi-stationary state (Figure 3b), which is, depending on temperature, a combination of WS and SS states. Of course, no signal for this quasi-stationary state will be observed in TR EPR similar to the steady-state EPR signal, but the nanosecond spin dynamics following the laser pulse is expected to be observed.

The second peculiarity expected for TR EPR of breathing crystals is that even a low-intensity laser pulse can heat the sample (microcrystals dispersed in glycerol) by a few degrees Kelvin, and it may take some measurable time (up to milliseconds) until the system returns back to the thermal equilibrium. It is well-known that in Boltzman equilibrium the EPR signal intensity is proportional to $\sim g\beta H/kT$, where $g\beta H$ is the electron Zeeman energy and $kT$ is the thermal energy. At high temperatures (e.g., room temperatures) an increase of $T$


dx.doi.org/10.1021/ja306467e | J. Am. Chem. Soc. 2012, 134, 16319−16326

by a few degrees would lead to a negligible change of EPR signal intensity (given approximately by $\Delta T/T$). However, if $T \approx 5$ K, heating by $\Delta T = 1$ K would change the microwave absorption by roughly 20%. If the relaxation to thermal equilibrium occurs on the nano- to microsecond time scale, an undesired TR EPR signal due to the heating−cooling cycles may be superimposed with the signal arising from photoswitching.

**TR EPR Spectra.** Figure 4a shows TR EPR spectra of $Cu(hfac)_2L^{Pr}$ detected at several time delays after the laser flash. The light wavelength $\lambda = 532$ nm, which is close to the maximum of the MLCT band of SS state (Figure 2), was used for photoexcitation (see Supporting Information for details). For convenience of interpretation, Figure 4b shows the simulated zero-harmonic CW EPR spectra of $Cu(hfac)_2L^{Pr}$ in SS ($D_{SS}$) and WS ($Q_{WS}$) states using the previously determined values of **g**-tensors.[22] The EPR spectrum is always contributed by the spin triad in SS or WS state (high-field region of the spectrum) and by the magnetically isolated Cu2 ions (low-field region; Figure 1a). In the WS state both signals significantly overlap, even at W-band.

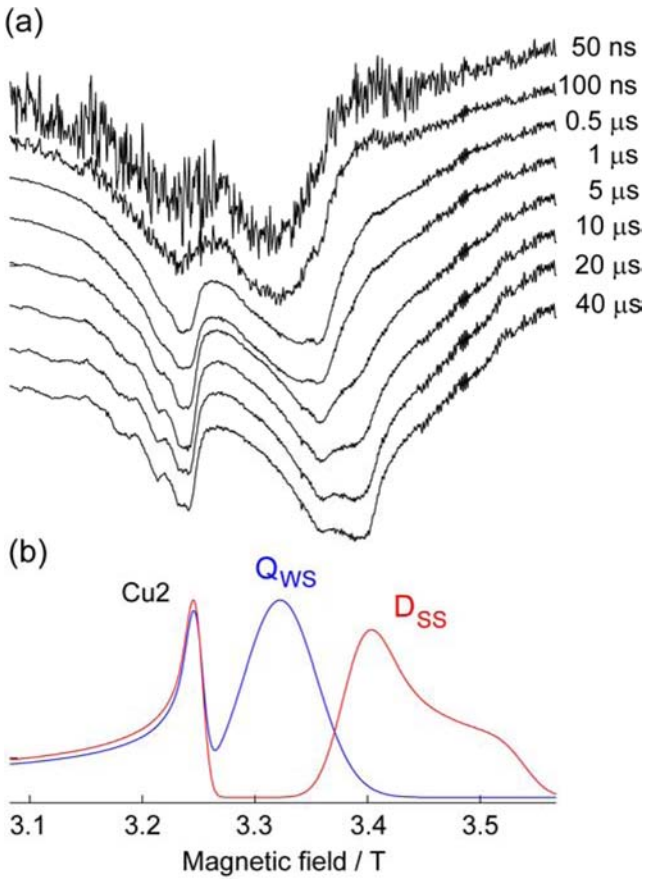


**Figure 4.** (a) W-band TR EPR spectra of the complex $Cu(hfac)_2L^{Pr}$ detected at different time delays after the laser flash (indicated on the right), $\nu_{mw} = 94.2$ GHz, $T = 7$ K. Spectra are normalized. (b) Calculated zero-harmonic EPR spectra of $Cu(hfac)_2L^{Pr}$ in SS (red line) and WS (blue line) states: $g_{eff}^{WS} = 2.03$; $g_{eff}^{SS} = [1.998, 1.983, 1.905]$; $g_{Cu2} = [2.075, 2.075, 2.371]$.

For interpreting CW EPR spectra of spin triads coupled by a strong exchange ($|J| > kT$), it is reasonable to consider only the ground spin multiplets of SS and WS states ($D_{SS}$ and $Q_{WS}$) and neglect the populations of other excited multiplets ($Q_{SS}$, $D_{WS}$, and $d_{SS,WS}$). However, in TR EPR experiments, one should also consider the possibility of detecting transient signals of these excited states. It is reasonable to assume that **g**-tensors of $D_{WS}$ and $D_{SS}$ states have close values (see Supporting Information); therefore, their transient signals should be found in the same spectral region and may be difficult to distinguish (the same holds for $Q_{WS}$ and $Q_{SS}$ states). Thus, until the final assignment to WS or SS state is made, we will refer to the observed signals simply as D and Q.

One can see that the spectra in Figure 4a resemble those in Figure 4b by shape, but the whole spectrum appears in negative ("emissive") phase. Moreover, the line of the magnetically isolated copper ion (Cu2) is clearly present in the spectrum, even though no spin state switching occurs under illumination with light in these coordination units. Thus, we clearly observe the strong undesired heating effect operating for both one-spin units and spin triads (see Supporting Information for additional confirmation). Since heating leads to a decrease of the EPR signal according to $\sim g\beta H/kT$, the phase of the TR EPR spectrum produced by it should be negative, as is observed in experiment.

At the same time, fortunately we also observe a change in the shape of the spectrum depending on the time delay after the flash. This cannot result from heating−cooling cycles, since certainly the spectrum decay due to the cooling must be homogeneous across the whole spectrum. It is also evident that the changes in the shape of the spectrum occur around the positions of EPR lines of the spin triad in SS and WS states. Therefore, these changes should be assigned to the effect of photoswitching and subsequent relaxation in spin triads.

**TR EPR Kinetics.** Although the heating/cooling effect makes the dominant contribution to the TR EPR signal, the less pronounced effect of photoswitching can easily be separated. Since heating and cooling occur identically in spin triads and one-spin copper units, the TR EPR kinetics measured on the EPR line of the one-spin copper unit (Cu2) fully describes the time profile of heating and cooling ($I_{Cu2}^{obs}(t) = I_{heat}(t)$). The observed kinetics measured at field positions corresponding to $Q_{WS}$ and $D_{SS}$ states of spin triads can be written in the following form:

$$I_Q^{obs}(t) = I_Q(t) + a_Q I_{heat}(t) \quad (1)$$

$$I_D^{obs}(t) = I_D(t) + a_D I_{heat}(t)$$

where $I_Q(t)$ and $I_D(t)$ are the spin-state switching kinetics of $Q_{WS}$ and $D_{SS}$ states, and $a_Q$ and $a_D$ are the corresponding coefficients of proportionality for the contribution of heating/cooling effects on those spin triads that do not undergo photoswitching.

Figure 5 shows the TR EPR kinetics of the one-spin copper ion Cu2 and the triad in D and Q states at two different temperatures. It is evident that the shapes of the curves differ only at short time delays of less than ~15 μs, implying that all processes associated with photoswitching occur within ~15 μs, and at longer time delays the signal is determined purely by the cooling effect. Therefore, in order to get rid of the unknowns $a_Q$ and $a_D$, all three observed TR EPR kinetics $I_{Cu2}^{obs}(t)$, $I_Q^{obs}(t)$, and $I_D^{obs}(t)$ can be normalized at $t > 15$ μs. Indeed, this approach works well, as is shown in Figure 5. After normalization at $t >$ 15 μs, heating/cooling kinetics can be subtracted from $I_Q^{obs}(t)$ and $I_D^{obs}(t)$ to obtain $I_Q(t)$ and $I_D(t)$. Note that $I_Q(t)$ and $I_D(t)$ are not really pure kinetics of spin state switching; in fact, they


dx.doi.org/10.1021/ja306467e | J. Am. Chem. Soc. 2012, 134, 16319−16326

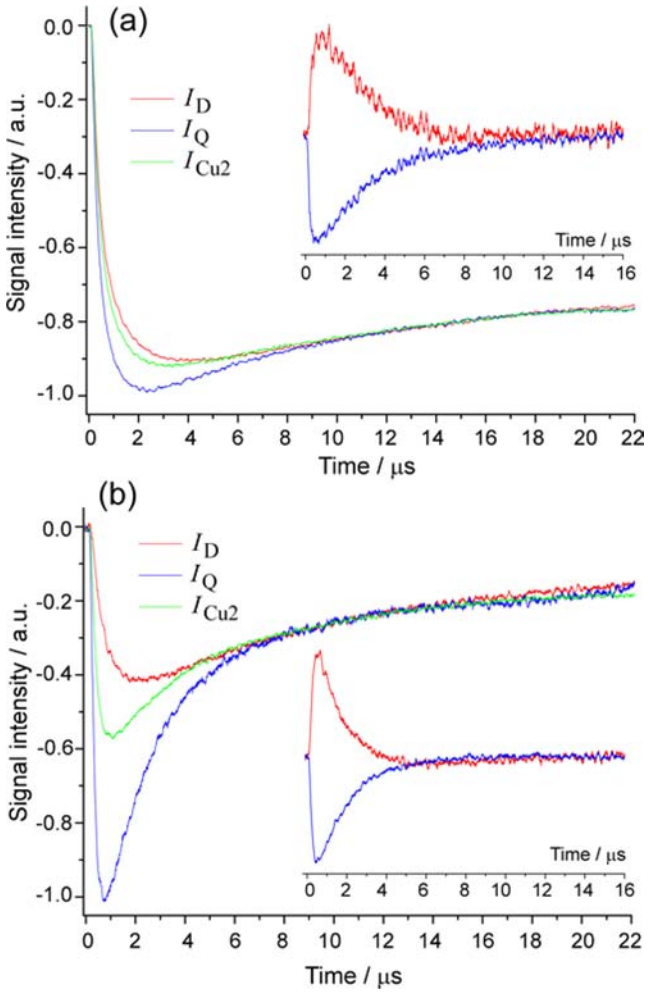


**Figure 5.** TR EPR kinetics of $Cu(hfac)_2L^{Pr}$ measured in the field positions corresponding to one-spin copper ion (Cu2) and spin triad in D and Q states (3.234, 3.426, and 3.318 T, respectively), at (a) 5 and (b) 11 K. The kinetics are normalized at $t > 15$ μs. Insets show corresponding pure TR EPR kinetics of D and Q states after subtraction of the heating/cooling effect and normalization.

also contain a contribution from heating and cooling during photoswitching and relaxation. However, this contribution is negligible because (i) the effect of heating is only a few percent for a given spin, as discussed above, and (ii) cooling kinetics is much slower than the excited state relaxation, as also is discussed above. Therefore, we may consider the result of subtraction shown in the insets of Figure 5 as a pure effect of photoswitching.

It is clear that the effect of heating is much more pronounced at 5 K compared to 11 K, because the difference between observed kinetics $I_{Cu}^{obs}(t)$, $I_Q^{obs}(t)$, and $I_D^{obs}(t)$ at 5 K is much smaller. This is, again, in good agreement with the above arguments that the EPR signal intensity ($\propto g\beta H/kT$) changes to the larger extent when the same heating occurs at 5 K compared to 11 K ($\Delta T/T$ is larger at 5 K for the same $\Delta T$).

The characteristic rise time of the kinetics is about 100−150 ns after the laser flash, and this time does not change noticeably between 5 and 21 K. In principle, the initial build-up of TR EPR kinetics can be determined by a number of factors, including (i) the formation time of paramagnetic intermediates, (ii) finite relaxation times, and (iii) characteristic time of the detection system response, determined by the $Q$-factor of the resonator and bandwidth of the preamplifier. As was mentioned above, the relaxation times in breathing crystals are extremely short. In addition, the rise of the TR EPR kinetics does not depend on the amplitude of the microwave field $B_1$ that would be expected for hypothesis (ii) (see Supporting Information). The response time in our experiments was estimated to be ∼100 ns; therefore, it can well be the major factor determining the kinetics build-up. Thus, the light-induced state is formed at time delays shorter than 100 ns.

The shapes of the TR EPR kinetics of WS and SS states coincide within experimental accuracy, whereas the sign of the kinetics is different, meaning that we indeed observe the interconversion between these two states. The validity of normalization and subtraction procedures can also be cross-checked by comparison of the kinetics $I_Q(t)$ and $I_D(t)$ with the difference kinetics $I_{diff}(t) = I_Q^{obs}(t) - I_D^{obs}(t)$. Once $I_Q^{obs}(t)$ and $I_D^{obs}(t)$ are normalized at $t > 15$ μs, the heating/cooling contribution is eliminated by subtraction, $I_Q^{obs}(t) - I_D^{obs}(t)$, to obtain $I_{diff}(t)$. Remarkably, the decays of all kinetics $I_Q(t)$, $I_D(t)$, and $I_{diff}(t)$ coincide within experimental accuracy (Figure 6).

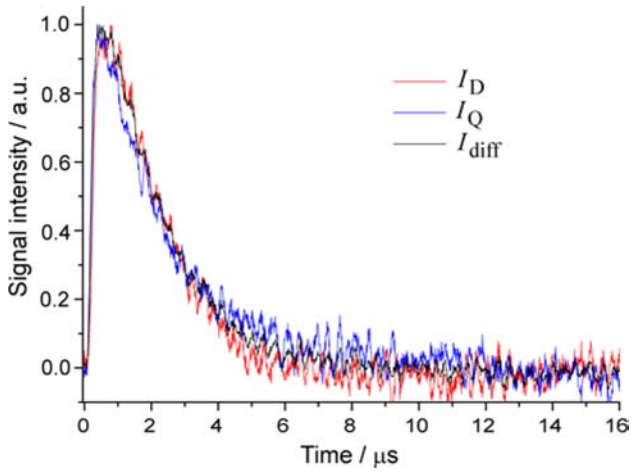


**Figure 6.** Comparison of TR EPR kinetics $I_Q(t)$, $I_D(t)$, and $I_{diff}(t)$, obtained at 7 K after the subtraction of heating/cooling kinetics. All kinetics are normalized to their maxima.

Theoretically, the magnetic susceptibility (and the second integral over the EPR spectrum) of the spin triad in WS state is larger compared to that in SS state by a factor close to 3.[22] But the widths and shapes of the corresponding EPR spectra are different; therefore, it is difficult to predict the expected ratio for the amplitudes of $I_Q(t)$ and $I_D(t)$ dependences. It was found experimentally that $I_Q(t) \approx -I_D(t)$, and, as a result, $I_{diff}(t) \approx 2\,I_Q(t)$, which gives a ∼2-fold increase in the signal intensity.

**Formation and Relaxation of Photoinduced State.** Our previous studies have shown that illumination with light at $T$ = 5−21 K (ground state is SS state) results in formation of the metastable WS state and its relaxation to the ground state on the time scale of hours (Figure 1b, direct conversion).[26,27] Therefore, one would expect to observe the formation of WS state from SS state on the nanosecond time scale of TR EPR. However, contrary to this expectation, the observed pure photoswitching kinetics of the $Q_{WS}$ state $I_Q(t)$ is emissive, meaning that light converts some fraction of the WS states to SS states. In agreement with this, the kinetics of the $D_{SS}$ state $I_D(t)$ is absorptive, meaning that some fraction of SS states was born by light illumination of the WS states.


dx.doi.org/10.1021/ja306467e | J. Am. Chem. Soc. 2012, 134, 16319−16326

As was already mentioned above, the TR EPR experiment requires a long accumulation time and WS→SS relaxation is slow; therefore, the system relaxes only to some quasi-stationary state between the laser flashes (Figure 3b), i.e., an equilibrium between photoinduced and relaxing WS state and ground SS state. Since the concentration of WS state is nonzero before every laser flash, the reverse conversion from WS to SS state found on the nanosecond time scale by TR EPR is not impossible. Moreover, careful analysis shows that the amplitude of TR EPR kinetics ($I_Q(t)$ and $I_D(t)$) is closely proportional to the quasi-stationary concentration of WS state at each temperature between 5 and 21 K.

Thus, within the time window between two laser flashes, there must exist two opposite conversion trends (Figure 1b). The main process that was investigated previously by CW EPR is the "direct" conversion from the ground SS state to the metastable WS state that relaxes back on the time scale of hours via quantum tunneling. Since we apply TR EPR in quasi-stationary condition (Figure 3b), each laser shot must convert some fraction of SS state into the WS state to compensate for the same amount of the relaxed WS fraction since the previous flash. This direct SS→WS conversion pathway is not observed in our TR EPR experiments. At the same time, the opposite, "reverse" conversion WS→SS occurs on the time scale of <100 ns, followied by relaxation to the metastable WS state within ca. 1−2 $\mu$s. The UV−vis−near-IR absorption bands of WS and SS states strongly overlap, and even at $\lambda$ = 532 nm the absorbance in these states differs by less than a factor of 2 at $T$ = 80−300 K (Figure 2); therefore, simultaneous excitation of WS and SS states is inevitable. It was not understood before the present TR EPR study why this overlap does not destroy direct conversion from SS to WS state by inducing the opposite WS→SS conversion. Now we observe that some fraction of WS state seems to be converted to SS state at the short time delays but then quite rapidly relaxes back to the metastable WS state. But how can this relaxation happen if the SS state is the ground state with much lower energy than the WS state?

We suppose that the observed transient signal on the EPR line of the D state corresponds to the excited doublet state in WS state potential well ($D_{WS}$), not to the ground doublet state in SS state potential well ($D_{SS}$) (Figure 1b). As was mentioned above, both doublets ($D_{WS}$ and $D_{SS}$) should have the same or very close magneto-resonance parameters and therefore similar EPR spectra. The observed relaxation times of ca. 1−2 $\mu$s are quite reasonable for the electron relaxation times of the photoexcited spin states at low temperatures.[39,58] Thus, using TR EPR, we observe the "secondary" process of photo-excitation and relaxation in the WS state potential well. But why is the expected direct process of $D_{SS}$→$Q_{WS}$ conversion not visible? In fact, the efficiency of photoswitching per one laser shot is not high for the bulk sample we study, and it takes several minutes of illumination with 10−20 Hz frequency to reach the quasi-stationary condition.[27] Therefore, it is possible that the efficiency of the secondary process that we observe is higher, and therefore the direct process is simply not seen. Another possibility is that the direct process occurs on a time scale shorter than 100 ns, and the kinetics build-up due to this process is masked by resonator response function (in fact, similar to the observed secondary process), whereas the kinetics decay due to the tunneling is too slow to be detected with good sensitivity in TR EPR.

What can we learn from this secondary process? First, the lifetime of the excited E* state is shorter than our temporal resolution (~100 ns), since the formation of $D_{WS}$ state has no time lag with respect to the disappearance of the $Q_{WS}$ state. Second, since we observe an interconversion between only two states $D_{WS}$↔$Q_{WS}$ in TR EPR without noticeable additional relaxation pathways, we assume that the relaxation pathway E*→$D_{WS}$ is strongly preferred compared to the E*→$D_{SS}$,$Q_{SS}$ pathways. As was already mentioned above, this explains why the direct SS→WS conversion occurs efficiently despite the fact that absorption bands of SS and WS states strongly overlap.

We also can study the electron spin relaxation $D_{WS}$→$Q_{WS}$ in more detail by measuring its rate as a function temperature (Figure 7). Unfortunately, signal intensity drops rapidly with

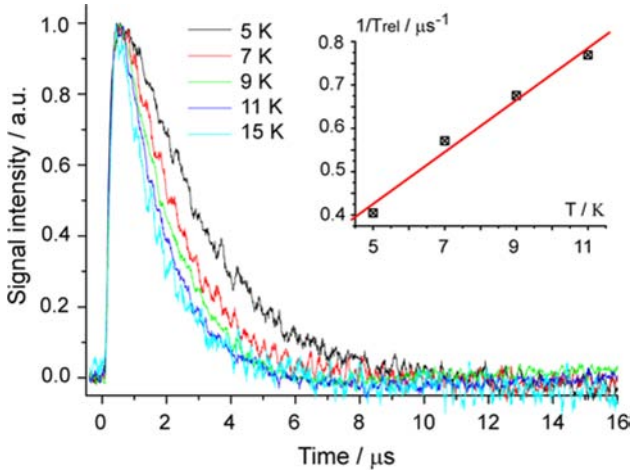


**Figure 7.** Temperature dependence of the observed relaxation kinetics between $D_{WS}$ and $Q_{WS}$ states at $T$ = 5−15 K. Inset: Relaxation rate ($1/T_{rel}$) vs $T$. Red line shows linear fit of the data using the equation $1/T_{rel}$ = 0.12 + 0.06$T$ $\mu s^{-1}$.

temperature; therefore, reliable data on the relaxation times can only be obtained within a narrow range of 5−11 K. In this region the relaxation rate depends linearly on temperature, implying a direct relaxation process.[59] The splitting between quartet and upper doublet of the triad in WS state ($Q_{WS}$ and $D_{WS}$) is expected to be about 10−30 $cm^{-1}$,[25] typical for the elongated octahedral geometry with radical spins in the axial positions.[57,60,61] Therefore, this splitting is close to the maximum of the phonon density spectrum at $T \approx$ 5−20 K, and one would not expect the dominating role of two-phonon processes. Possibly, this relaxation transition $D_{WS}$→$Q_{WS}$ can be caused by modulation of anisotropic exchange coupling[56] or other weakly allowed processes between these two states.

The results reported above show both similarities and differences between light-induced phenomena in copper−nitroxide-based breathing crystals compared to iron(II) LIESST compounds. The mechanism of LIESST in iron(II) SCO compounds was elucidated in detail during the past several decades.[62] In particular, it has been shown that excitation occurs via d−d or MLCT absorption bands of the low-spin ground state, and that the formation of the excited high-spin state is ultrafast (time scale ~$10^{-13}$−$10^{-10}$ s).[62−64] Demanding optical properties of breathing crystals Cu(hfac)$_2$$L^R$ (overlap of UV−vis absorption spectra of the ground and excited states) strongly complicate the study of the mechanism of light-induced spin state switching. One way to overcome this difficulty is to design breathing crystals with another type of stable radical having more suitable optical properties, and we


dx.doi.org/10.1021/ja306467e | J. Am. Chem. Soc. 2012, 134, 16319−16326

have already obtained some successful results in this direction;[65] the studies of light-induced phenomena in new group of compounds are underway. Another way to obtain missing information on light-induced dynamics in breathing crystals is to involve more sophisticated physical techniques, e.g., as was done in the present work using TR EPR. We could see that, similar to iron(II) LIESST compounds, the formation of the photoinduced state is fast (<100 ns) and the relaxation from the intermediate excited state is strongly preferred toward the photoinduced (WS) state. At the same time, light-induced spin dynamics in breathing crystals is more complicated compared to that in iron(II) compounds because of the presence of low-lying excited spin levels (excited multiplets of exchange-coupled spin triads nitroxide−copper(II)−nitroxide). In particular, TR EPR allowed us to study the electron spin relaxation between excited and ground spin multiplets of the WS state. TR EPR studies with higher sensitivity and higher spectral and temporal resolution may lead to further advancement in the determination of the detailed mechanism of photoswitching in breathing crystals.

## CONCLUSIONS

In this work we have studied light-induced spin dynamics on the nanosecond time scale in a compound of the "breathing crystals" family using W-band time-resolved EPR. Although TR EPR is widely used for studying photoinduced transient paramagnetic intermediates in liquid/frozen solutions, to the best of our knowledge, it has never before been applied to solid-phase (magnetically concentrated) switchable molecular magnets. The potential of TR EPR applied to these and similar photoswitchable systems has been demonstrated. We have found that "direct" conversion from SS to WS state is not visible in TR EPR experiments, and the observed spectra and kinetics characterize "secondary" processes of initiation and relaxation of the excited doublet spin state in the potential well of the metastable WS state. The formation of this state occurs during a time of less than ∼100 ns. The reverse relaxation to the ground spin multiplet of the WS state occurs on the time scale of several microseconds and has an exponential character. The temperature dependence of the relaxation rate is linear at $T$ = 5−11 K, implying a direct relaxation process. The observation of a secondary excitation/relaxation pathway in the WS state unveils some properties of the intermediate light-induced state involved in both direct and secondary conversion routes. In particular, relaxation from this state has a strong preference toward the metastable WS state. This explains why direct SS→WS conversion is overall efficient despite the strong overlap of UV−vis−near-IR absorption bands of WS and SS states. Although the detailed photoswitching mechanism in breathing crystals is still not understood, this first high-resolution W-band TR EPR study opens the perspective for the future investigations of the spin state conversion and understanding of the underlying mechanisms of photoinduced phenomena in these and similar systems.

## ASSOCIATED CONTENT

### Supporting Information

(1) Brief overview of synthesis, structure, magnetic properties, and EPR data of the complex $Cu(hfac)_2L^{Pr}$ obtained previously; (2) LIESST observation in $Cu(hfac)_2L^{Pr}$ using illumination with $\lambda$ = 532 nm light; (3) EPR spectra of $Cu(hfac)_2L^{Pr}$ embedded in PVC; (4) heating contribution dependence on laser intensity and temperature; (5) TR EPR kinetics at $T$ = 8 K measured at different microwave powers. This material is available free of charge via the Internet at http://pubs.acs.org.

## AUTHOR INFORMATION

### Corresponding Author

mfedin@tomo.nsc.ru; egbagryanskaya@nioch.nsc.ru

### Notes

The authors declare no competing financial interest.

## ACKNOWLEDGMENTS

This work was supported by the Russian Foundation for Basic Research (Nos. 11-03-00158, 12-03-31396, and 12-03-00067), the RF President's Grant (MK-1662.2012.3, MK-1165.2012.3), and RF Ministry of Education and Science (Nos. 8436 and 8456). E.G.B. thanks Tohoku University for financial support during her visit as an invited professor.

## REFERENCES

(1) Sauer, M. *Proc. Natl. Acad. Sci. U.S.A.* **2005**, *102*, 9433−9434.
(2) Browne, W. R.; Feringa, B. L. *Annu. Rev. Phys. Chem.* **2009**, *60*, 407−428.
(3) Coskun, A.; Banaszak, M.; Astumian, R. D.; Stoddart, J. F.; Grzybowski, B. A. *Chem. Soc. Rev.* **2012**, *41*, 19−30.
(4) Bousseksou, A.; Molnar, G.; Salmon, L.; Nicolazzi, W. *Chem. Soc. Rev.* **2011**, *40*, 3313−3335.
(5) Dei, A.; Gatteschi, D. *Angew. Chem., Int. Ed.* **2011**, *50*, 11852−11858.
(6) Sato, O.; Tao, J.; Zhang, Y.-Z. *Angew. Chem.* **2007**, *119*, 2200−2236; *Angew. Chem., Int. Ed.* **2007**, *46*, 2152−2187.
(7) Sessoli, R. *Nature Chem.* **2010**, *2*, 346−347.
(8) *Spin Crossover in Transition Metal Compounds I−III*, Topics in Current Chemistry *233−235*; Gütlich, P., Goodwin, H. A., Eds.; Springer-Verlag: Berlin/Heidelberg/New York, 2004.
(9) Decurtins, S.; Gutlich, P.; Kohler, C. P.; Spiering, H.; Hauser, A. *Chem. Phys. Lett.* **1984**, *105*, 1−4.
(10) Gutlich, P.; Hauser, A.; Spiering, H. *Angew. Chem., Int. Ed. Engl.* **1994**, *33*, 2024−2054.
(11) Chakraborty, P.; Bronisz, R.; Besnard, C.; Guénée, L.; Pattison, P.; Hauser, A. *J. Am. Chem. Soc.* **2012**, *134*, 4049−4052.
(12) Southon, P. D.; Liu, L.; Fellows, E. A.; Price, D. J.; Halder, G. J.; Chapman, K. W.; Moubaraki, B.; Murray, K. S.; Letard, J.-F.; Kepert, C. J. *J. Am. Chem. Soc.* **2009**, *131*, 10998−11009.
(13) Ono, K.; Yoshizawa, M.; Akita, M.; Kato, T.; Tsunobuchi, Y.; Ohkoshi, S.; Fujita, M. *J. Am. Chem. Soc.* **2009**, *131*, 2782−2783.
(14) Boldog, I.; Gaspar, A. B.; Martinez, V.; Pardo-Ibanez, P.; Ksenofontov, V.; Bhattacharjee, A.; Gutlich, P.; Real, J. A. *Angew. Chem., Int. Ed.* **2008**, *47*, 6433−6437.
(15) Duriska, M. B.; Neville, S. M.; Moubaraki, B.; Cashion, J. D.; Halder, G. J.; Chapman, K. W.; Balde, C.; Letard, J.-F.; Murray, K. S.; Kepert, C. J.; Batten, S. R. *Angew. Chem., Int. Ed.* **2009**, *48*, 2549−2552.
(16) Seredyuk, M.; Gaspar, A. B.; Ksenofontov, V.; Galyametdinov, Y.; Kusz, J.; Gutlich, P. *J. Am. Chem. Soc.* **2008**, *130*, 1431−1439.
(17) Cobo, S.; Ostrovskii, D.; Bonhommeau, S.; Vendier, L.; Molnar, G.; Salmon, L.; Tanaka, K.; Bousseksou, A. *J. Am. Chem. Soc.* **2008**, *130*, 9019−9024.
(18) Ikegami, K.; Ono, K.; Togo, J.; Wakabayashi, T.; Ishige, Y.; Matsuzaki, H.; Kishida, H.; Okamoto, H. *Phys. Rev. B* **2007**, *76*, 085106.
(19) Ovcharenko, V. I.; Maryunina, K. Yu.; Fokin, S. V.; Tretyakov, E. V.; Romanenko, G. V.; Ikorskii, V. N. *Russ. Chem. Bull., Int. Ed.* **2004**, *53*, 2406−2427.
(20) Ovcharenko, V. I.; Romanenko, G. V.; Maryunina, K. Yu.; Bogomyakov, A. S.; Gorelik, E. V. *Inorg. Chem.* **2008**, *47*, 9537−9552.
(21) Romanenko, G. V.; Maryunina, K. Yu.; Bogomyakov, A. S.; Sagdeev, R. Z.; Ovcharenko, V. I. *Inorg. Chem.* **2011**, *50*, 6597−6609.

(22) Fedin, M.; Veber, S.; Gromov, I.; Maryunina, K.; Fokin, S.; Romanenko, G.; Sagdeev, R.; Ovcharenko, V.; Bagryanskaya, E. *Inorg. Chem.* **2007**, *46*, 11405−11415.
(23) Veber, S. L.; Fedin, M. V.; Potapov, A. I.; Maryunina, K. Yu.; Romanenko, G. V.; Sagdeev, R. Z.; Ovcharenko, V. I.; Goldfarb, D.; Bagryanskaya, E. G. *J. Am. Chem. Soc.* **2008**, *130*, 2444−2445.
(24) Fedin, M. V.; Veber, S. L.; Maryunina, K. Yu.; Romanenko, G. V.; Suturina, E. A.; Gritsan, N. P.; Sagdeev, R. Z.; Ovcharenko, V. I.; Bagryanskaya, E. G. *J. Am. Chem. Soc.* **2010**, *132*, 13886−13891.
(25) Veber, S. L.; Fedin, M. V.; Maryunina, K. Yu.; Potapov, A.; Goldfarb, D.; Reijerse, E.; Lubitz, W.; Sagdeev, R. Z.; Ovcharenko, V. I.; Bagryanskaya, E. G. *Inorg. Chem.* **2011**, *50*, 10204−10212.
(26) Fedin, M.; Ovcharenko, V.; Sagdeev, R.; Reijerse, E.; Lubitz, W.; Bagryanskaya, E. *Angew. Chem., Int. Ed.* **2008**, *47*, 6897−6899; *Angew. Chem.* **2008**, *120*, 7003−7005.
(27) Fedin, M. V.; Maryunina, K. Yu.; Sagdeev, R. Z.; Ovcharenko, V. I.; Bagryanskaya, E. G. *Inorg. Chem.* **2012**, *51*, 709−717.
(28) Matsumoto, S.; Higashiyama, T.; Akutsu, H.; Nakatsuji, S. *Angew. Chem., Int. Ed.* **2011**, *50*, 10879−10883; *Angew. Chem.* **2011**, *123*, 11071−11075.
(29) Okazawa, A.; Ishida, T. *Inorg. Chem.* **2010**, *49*, 10144−10147.
(30) Setifi, F.; Benmansour, S.; Marchivie, M.; Dupouy, G.; Triki, S.; Sala-Pala, J.; Salaun, J.-Y.; Gomez-García, C. J.; Pillet, S.; Lecomte, C.; Ruiz, E. *Inorg. Chem.* **2009**, *48*, 1269−1271.
(31) Okazawa, A.; Hashizume, D.; Ishida, T. *J. Am. Chem. Soc.* **2010**, *132*, 11516−11524.
(32) Baskett, M.; Lahti, P. M.; Paduan-Filho, A.; Oliveira, N. F. *Inorg. Chem.* **2005**, *44*, 6725−6735.
(33) dePanthou, F. L.; Belorizky, E.; Calemczuk, R.; Luneau, D.; Marcenat, C.; Ressouche, E.; Turek, P.; Rey, P. *J. Am. Chem. Soc.* **1995**, *117*, 11247−11253.
(34) Caneschi, A.; Chiesi, P.; David, L.; Ferraro, F.; Gatteschi, D.; Sessoli, R. *Inorg. Chem.* **1993**, *32*, 1445−1453.
(35) Fessenden, R. W. *J. Chem. Phys.* **1973**, *58*, 2489−2500.
(36) Forbes, M. D. E. *Photochem. Photobiol.* **1997**, *65*, 73−81.
(37) Turro, N. J.; Kleinman, M. H.; Karatekin, E. *Angew. Chem., Int. Ed.* **2000**, *39*, 4436−4461.
(38) Kobori, Y.; Yago, T.; Akiyama, K.; Tero-Kubota, S. *J. Am. Chem. Soc.* **2001**, *123*, 9722−9723.
(39) Teki, Y.; Miyamoto, S.; Nakatsuji, M.; Miura, Y. *J. Am. Chem. Soc.* **2001**, *123*, 294−305.
(40) Brustolon, M.; Barbon, A.; Bortolus, M.; Maniero, A. L.; Sozzani, P.; Comotti, A.; Simonutti, R. *J. Am. Chem. Soc.* **2004**, *126*, 15512−15519.
(41) Schleicher, E.; Kowalczyk, R. M.; Kay, C. W. M.; Hegemann, P.; Bacher, A.; Fischer, M.; Bittl, R.; Richter, G.; Weber, S. *J. Am. Chem. Soc.* **2004**, *126*, 11067−11076.
(42) Poluektov, O. G.; Paschenko, S. V.; Utschig, L. M.; Lakshmi, K. V.; Thurnauer, M. C. *J. Am. Chem. Soc.* **2005**, *127*, 11910−11911.
(43) Akiyama, K.; Hashimoto, S.; Tojo, S.; Ikoma, T.; Tero-Kubota, S.; Majima, T. *Angew. Chem., Int. Ed.* **2005**, *44*, 3591−3594.
(44) Chernick, E. T.; Mi, Q.; Kelley, R. F.; Weiss, E. A.; Jones, B. A.; Marks, T. J.; Ratner, M. A.; Wasielewski, M. R. *J. Am. Chem. Soc.* **2006**, *128*, 4356−4364.
(45) Concepcion, J. J.; Brennaman, M. K.; Deyton, J. R.; Lebedeva, N. V.; Forbes, M. D. E.; Papanikolas, J. M.; Meyer, T. J. *J. Am. Chem. Soc.* **2007**, *129*, 6968−6969.
(46) Kobori, Y.; Shibano, Y.; Endo, T.; Tsuji, H.; Murai, H.; Tamao, K. *J. Am. Chem. Soc.* **2009**, *131*, 1624−1625.
(47) Giacobbe, E. M.; Mi, Q.; Colvin, M. T.; Cohen, B.; Ramanan, C.; Scott, A. M.; Yeganeh, S.; Marks, T. J.; Ratner, M. A.; Wasielewski, M. R. *J. Am. Chem. Soc.* **2009**, *131*, 3700−3712.
(48) Lebedeva, N. V.; Tarasov, V. F.; Resendiz, M. J. E.; Garcia-Garibay, M. A.; White, R. C.; Forbes, M. D. E. *J. Am. Chem. Soc.* **2010**, *132*, 82−84.
(49) Kobori, Y.; Fuki, M. *J. Am. Chem. Soc.* **2011**, *133*, 16770−16773.
(50) Colvin, M. T.; Ricks, A. B.; Scott, A. M.; Smeigh, A. L.; Carmieli, R.; Miura, T.; Wasielewski, M. R. *J. Am. Chem. Soc.* **2011**, *133*, 1240−1243.
(51) Berthold, T.; Donner von Gromoff, E.; Santabarbara, S.; Stehle, P.; Link, G.; Poluektov, O. G.; Heathcote, P.; Beck, C. F.; Thurnauer, M. C.; Kothe, G. *J. Am. Chem. Soc.* **2012**, *134*, 5563−5576.
(52) Biskup, T.; Hitomi, K.; Getzoff, E. D.; Krapf, S.; Koslowski, T.; Schleicher, E.; Weber, S. *Angew. Chem., Int. Ed.* **2011**, *50*, 12647−12651.
(53) Ovcharenko, V. I.; Fokin, S. V.; Romanenko, G. V.; Shvedenkov, Yu. G.; Ikorskii, V. N.; Tretyakov, E. V.; Vasilevsky, S. F. *J. Struct. Chem.* **2002**, *43*, 153−169.
(54) Stoll, S.; Schweiger, A. *J. Magn. Reson.* **2006**, *178*, 42−55.
(55) Fedin, M.; Veber, S.; Gromov, I.; Ovcharenko, V.; Sagdeev, R.; Schweiger, A.; Bagryanskaya, E. *J. Phys. Chem. A* **2006**, *110*, 2315−2317.
(56) Fedin, M.; Veber, S.; Gromov, I.; Ovcharenko, V.; Sagdeev, R.; Bagryanskaya, E. *J. Phys. Chem. A* **2007**, *111*, 4449−4455.
(57) Allao, R.; Jordao, A.; Resende, J.; Cunha, A.; Ferreira, V.; Novak, M.; Sangregorio, C.; Sorace, L.; Vaz, M. *Dalton Trans.* **2011**, *40*, 10843−10850.
(58) Yamauchi, S.; Takahashi, K.; Islam, S. S. M.; Ohba, Y.; Tarasov, V. *J. Phys. Chem. B* **2010**, *114*, 14559−14563.
(59) Abragam, A.; Bleaney, B. *Electron Paramagnetic Resonance of Transition Ions*; Oxford University Press: London, 1970.
(60) Benelli, C.; Gatteschi, D.; Zanchini, C.; Latour, J. M.; Rey, P. *Inorg. Chem.* **1986**, *25*, 4242−4244.
(61) Musin, R. N.; Schastnev, P. V.; Malinovskaya, S. A. *Inorg. Chem.* **1992**, *31*, 4118−4121.
(62) Hauser, A. In *Spin Crossover in Transition Metal Compounds II*, Topics in Current Chemistry *234*; Gütlich, P., Goodwin, H. A., Eds.; Springer-Verlag: Berlin/Heidelberg, 2004; pp 155−198.
(63) Cannizzo, A.; Milne, C. J.; Consani, C.; Gawelda, W.; Bressler, Ch.; van Mourik, F.; Chergui, M. *Coord. Chem. Rev.* **2010**, *254*, 2677−2686.
(64) Collet, E.; Moisan, N.; Balde, C.; Bertoni, R.; Trzop, E.; Laulhe, C.; Lorenc, M.; Servol, M.; Cailleau, H.; Tissot, A.; Boillot, M.-L.; Graber, T.; Henning, R.; Coppens, P.; Buron-Le Cointea, M. *Phys. Chem. Chem. Phys.* **2012**, *14*, 6192−6199.
(65) Fedin, M. V.; Drozdyuk, I. Yu.; Tretyakov, E. V.; Tolstikov, S. E.; Ovcharenko, V. I.; Bagryanskaya, E. G. *Appl. Magn. Reson.* **2011**, *41*, 383−392.